TOWARD AN IN-DEPTH MATERIAL MODEL FOR CERMET NUCLEAR THERMAL ROCKET FUEL ELEMENTS

William C. Tucker,[a]* Piyas Chowdhury,[a] Lauren J. Abbott,[b] and Justin B. Haskins[b*]

[a]*AMA, Inc., Thermal Protection Materials Branch, NASA Ames Research Center, Moffett Field, CA, 94035, USA*

[b]*Thermal Protection Materials Branch, NASA Ames Research Center, Moffett Field, CA, 94035, USA*

*E-mail: william.c.tucker@nasa.gov, justin.b.haskins@nasa.gov

TOWARD AN IN-DEPTH MATERIAL MODEL FOR CERMET NUCLEAR THERMAL ROCKET FUEL ELEMENTS

The development and qualification of nuclear thermal propulsion (NTP) fuel element technologies would be aided by an in-depth model of material response and failure modes at operating conditions. Integrated computational materials engineering techniques have the potential to provide such a model, as demonstrated here through three case studies focused on a tungsten-uranium mononitride cermet fuel. The first case focuses on the erosion of tungsten (W, also named wolfram), a nominal coating/cladding and fuel element matrix material, in hot hydrogen. Ab initio techniques are used to calculate erosion rates and thermal expansion at NTP operating conditions. The second focuses on the stability of uranium mononitride (UN) fuels at high temperature and in the presence of hydrogen. Phase diagram techniques augmented with ab initio thermodynamic data reveal potential instabilities and decomposition pathways at high hydrogen concentrations. The third focuses on using microstructure information to predict high temperature mechanical response and failure of tungsten. Combined finite element and discrete dislocation dynamics techniques provide mechanical properties in agreement with experimental methods. The integration of these techniques for an all-encompassing material model is discussed.

Keywords: cermet; modeling; mechanical; chemical; erosion

I. INTRODUCTION

Nuclear thermal propulsion (NTP) offers benefits over conventional chemical propulsion, such as a higher specific impulse (I_{sp} ~ 900 s, a factor of ~2 better), a higher thrust to mass ratio, better tolerance to payload mass growth and architecture, and lower initial mass in low-Earth orbit. As these benefits could lead to a reduction in heavy lift launch count, cost, and risk,[1,2] NTP is now being considered for faster transit for manned missions to Mars and beyond as well as for commercial missions to the Moon.[3]

The canonical version of an NTP rocket (Fig. 1a) has a solid fuel element that is composed of a matrix material containing uranium ceramic fuel particles and has

longitudinal channels running through the fuel element that allow thermal energy generated from nuclear reactions to directly heat the hydrogen (H_2) propellant, which is exhausted for propulsion (Fig. 1b). During operation, the fuel element can reach temperatures ranging from 2400 to 2750 K, or even over 3000 K in some currently proposed designs.[3,4] These temperatures are much higher than those found in typical power plant reactors, and the presence of cryogenic hydrogen leads to large thermal gradients across the elements. Additionally, the reactor must be operated cyclically for many hours. These factors lead to a host of challenges related to the thermal, mechanical, and chemical stability of NTP fuel elements during operation.[5] Thus, material selection and characterization play a critical role to enabling this technology.

The earliest exploration of NTP rockets occurred through Project Rover and NASA's Nuclear Engine for Rocket Vehicle Application (NERVA) program from 1955-1972. These efforts resulted in rocket ground tests that provided a unique wealth of information related to the performance of fuel elements with graphite matrix material in extreme thermal and fission environments. In parallel with the Project Rover/NERVA efforts, Argonne National Laboratory (ANL)[6] and General Electric (GE)[7] worked on fuel elements that used ceramic-metal (cermet) fuel, composed of a metal matrix with a fissile uranium ceramic, UO_2, embedded sporadically within. Similar factors were identified in both material architectures that reduced the useful lifetime of the fuel elements. One such factor was instability in the propellant channel coatings and claddings during operation due to thermal expansion mismatch, which caused cracking when thermally cycled.[5] Such cracking allowed greater diffusion of hydrogen into the metal matrix material and increased the likelihood of degradation of the UO_2ceramic. Another factor was

mechanical instability of UO_2, which caused cracking during thermal cycling and again led to hydrogen degradation of the matrix material.[5]

Despite these challenges, the Project Rover/NERVA efforts were deemed successful based on numerous rocket ground tests, but they were ultimately cancelled due to budget challenges. Mission concepts and feasibility studies[1,3] focused on realizing this technology have arisen periodically over the half century since. Unfortunately, none of these studies progressed to the point of full scale ground testing in NTP thermal and fission environments like the original efforts.

More recently, interest in NTP has reignited, with a notable effort being undertaken at NASA to improve the stability of fuel elements.[8-10] A particular focus has been on cermet fuels having tungsten claddings and tungsten-based metal matrix alloys and UN ceramics.[9] Relatedly, tungsten also serves as a prototype coating for propellant channels in carbide or oxide substrates due to its resistance to hydrogen infiltration. For this reason tungsten is an ideal material for the manufacture of plasma-facing components in fusion reactors, and the interaction of hydrogen isotopes with tungsten is a current area of research.[11] A variety of ceramic uranium (U) fuels can be considered for these systems, including uranium oxide (UO_2), uranium carbide (UC), and uranium mononitride (UN).[10] Though a pure tungsten fuel element matrix is not neutronically ideal and must be alloyed, understanding the reactivity of tungsten and the various uranium-based ceramics with hydrogen, the proposed propellant, is critical.

Many of the material issues faced by the early NTP development efforts could have been more quickly identified and remedied by integrating the in-depth material modeling capabilities available today, which would have reduced the costly trial-and-error development with experimental fabrication and testing in hot hydrogen. Namely, integrated computational materials engineering (ICME) techniques, which span the

atomistic scale (e.g., *ab initio* and molecular dynamics), mesoscale/microscale (e.g., discrete dislocation dynamics), and the macroscale (e.g., finite element), have shown promise for characterizing materials in extreme conditions.[12-16] For ceramic uranium materials, *ab initio* (specifically density functional theory) computations have been used to predict crystal structural characteristics, vibrational spectra, mechanical properties, and thermodynamic properties at a range of temperatures with comparable accuracy to experiments.[12-13] For refractory metals like tungsten, discrete dislocation dynamics have shown the ability to provide experimentally comparable measures of mechanical response and plasticity in single crystals.[15,16] The success of such methods implies possible applications to other aspects of fuel element material behavior, such as the susceptibility of materials to hydrogen reactions and vaporization, intercalation and mobility of hydrogen or fission species into coatings and substrates, creep and hydrogen embrittlement effects on mechanical performance, and fracture in fuel materials.

Thus, the present work aims to demonstrate the utility of ICME techniques for contemporary cermet fuel elements. The specific focus is on a hypothetical W-UN architecture. Three cases are investigated, with the focus of each being aligned with long-standing challenges noted from the early efforts of Project Rover/NERVA, ANL, and GE. (1) Case one focuses on the erosion of tungsten cladding material by hot hydrogen. Specifically, *ab initio* simulations are performed to determine the preferred mechanism of vacuum mas loss. High temperature thermal expansion coefficients (CTEs) are also calculated. (2) Case two focuses on the phase stability of uranium mononitride in the presence of hot hydrogen. In this case, *ab initio* computations coupled to thermodynamic procedures provide reaction Gibbs free energies that quantify the temperature ranges where hydrogen-mediated degradation of uranium mononitride is expected. (3) Case three investigates the mechanical properties of tungsten microstructures. Discrete

dislocation dynamics simulations provide a means of characterizing stress distributions to predict cracking in tungsten and quantifying plasticity present in macroscale stress-strain curves. Each of the three cases provides unique information that can be used to better characterize fuel element material performance and failure modes.

II. METHODS

II.A. Ab Initio Computations and Simulations

Ab initio density functional theory (DFT) computations are used to understand the chemical reactions of tungsten and uranium mononitride at the atomic scale with hot hydrogen to elucidate degradation mechanisms. Such computations were performed with the Vienna Ab Initio Simulation Package (VASP).[17] VASP is a plane-wave electronic structure code that solves the Kohn-Sham equations to inform material energetics and, *via* the quasi-harmonic approximation (QHA) performed with the Phonopy[18] software package, basic thermodynamic properties. All calculations were performed using the VASP-recommended PBE pseudopotentials for W, U, N, and H.[19]

For tungsten coatings/claddings simulated in Case 1, 4-layer slabs were generated by terminating bcc supercells along the (110) plane, the lowest energy surface for W, and interactions with hydrogen were examined at the surface. The primary mechanism for coating and substrate vacuum erosion mass loss will be attributed to chemical reactions with atomic hydrogen and the subsequent formation of gaseous refractory products. To examine this phenomenon, the Gibbs free energies of the various solid materials under consideration must be obtained, along with the free energies of possible gaseous hydrogenated refractory molecules. The free energies can be used to derive equilibrium constants for reactions that will inform the loss of material, given that equilibrium is met.

For the uranium nitride reactants and products in Case 2, uranium mononitride (UN), a leading fuel candidate for nuclear thermal rockets, uranium sesquinitride (U_2N_3),

tetrauranium heptanitride (U_4N_7), and uranium hydride (UH_3) were considered; all of these materials are stable and have been observed experimentally. [20] The crystal structures for UN and U_2N_3 were obtained from previous DFT investigations of electronic structure.[21-24] The structure of U_4N_7 is predicted and obtained from the Materials Project database,[23] as experimental structural characterization is primarily limited to lattice constants.[25] The calculations were performed using the guidelines in the work of Gryaznov and coworkers,[26] which consists of using DFT+U with a U value of 1.85 eV and the neglect of magnetism to approximate the high-temperature paramagnetic states of the uranium compounds. Spin-orbit coupling was shown in previous electronic computations to have a minor effect on relative energetics and is thus neglected.[24,26] Phase calculations were based upon simple Gibbs energy comparisons using data from DFT and Phonopy, with experimental data for H/H2. These data were collated in an Excel spreadsheet and compared with each other.

II.B. Microscale Mechanical Modeling

To evaluate the mechanical response and failure initiation of polycrystalline microstructures, the Dusseldorf Advanced Material Simulation Kit (DAMASK)[27] is employed. In contrast to VASP's atomic-scale simulations, DAMASK is a highly modular freeware code for modeling materials structure-property relationships at the grain/micron scale with different types of mechanistic constitutive laws and numerical solvers. It is designed to accurately correlate microscopic phenomena (e.g. plastic deformation, phase transformation, hydrogen embrittlement, micro-cracking, or irradiation damage) with macro-scale responses. For the present work, DAMASK is employed to study the microscopic damage evolution in tungsten under the operating conditions of NTP. Microstructures with 20 grains of an average diameter of 20 microns, representative of the typical grain size of additively manufactured tungsten,[28] on a

120x120x120 cubic grid were randomly generated via Voronoi tessellation. The stress/strain response was then calculated based on a relevant set of mechanical properties.[29]

III. RESULTS

III.A. Case 1: Substrate and Coating Stability and Erosion in Hydrogen

One objective related to the development of cermet fuels for NTP is to identify erosion mechanisms of the matrix and any potential claddings or coatings. The coating material must be of sufficient thickness to withstand erosion from hot hydrogen and protect the underlying cermet and must also exhibit thermal expansion characteristics consistent with the underlying substrate to avoid buckling and cracking along the interface. Additionally, any cracks in the coating will allow direct access of hydrogen to the core matrix substrate and lead to enhanced erosion. Thus, understanding the thermal expansion and loss of potential coating and matrix materials at given operation conditions (time, temperature, pressure) is critical.

Because accurate experimental databases of the thermodynamics for the various solid materials and gaseous products do not exist at the temperatures of interest, *ab initio* computations are performed to obtain free energies. These free energies were used to calculate the likelihood of various erosion mechanisms at high temperature. The schematic depicted in Fig. 2 demonstrates this ability. Here, three different erosion mechanisms of a tungsten surface are reported along with their likelihood of occurring at 2500 K. For simplicity of calculations, no flow of hydrogen was considered. Instead, the energetics of the process were calculated to provide an order of magnitude estimate of the erosive effect of both atomic and molecular hydrogen on an ideal W surface. Direct erosion of a W surface is shown to be far more unlikely than hydrogen-mediated erosion.

When H and H_2 are present, both aid the erosion significantly, with erosion by H being ~200 times more probable than by H_2. At elevated temperatures, much of the molecular hydrogen will have dissociated, and atomic hydrogen will thus be responsible for the majority of mass loss.

These thermodynamic calculations also enable the calculation of free-energy informed thermal expansion coefficients via the quasi-harmonic approximation.[18] After calculating free energies at varying volumes and temperatures, the linear coefficient of thermal expansion of tungsten was derived and is plotted in Fig. 3. The thermal expansion calculated here is that of monocrystalline bulk W, whereas real-world samples of W are almost always polycrystalline. Notably, the calculated values for monocrystalline W show good agreement between the moderately widespread values reported in literature.[30-33] Particularly, the increasing trend in thermal expansion with temperature most closely matches that of the ITER fusion energy consortium's values, [30] which were obtained via a more advanced experimental method, XRD, than those in earlier studies which utilized extensometers. [31-33] These results demonstrate an ability to predict potential buckling and erosion mechanisms at NTP operating temperatures.

III.B. Case 2: Fuel Chemical Stability in the Presence of Hydrogen

The stability of uranium fuels in high temperature fuel elements exposed to different levels of hydrogen is of crucial importance. The reaction of uranium-containing compounds to form the high specific-volume UH_3 can lead to internal stresses that promote fracture and eventually element failure as well as overall decreased control of the fission reaction.[34] The temperature and hydrogen concentration dependence of such reactions must be quantified to assess their prevalence in nuclear thermal rocket fuel

elements, which will be subjected to large thermal and hydrogen concentration fluctuations during cyclical operation.

The stability of UN, a leading candidate for use in tungsten-based cermets, is of primary interest in the present work. The crystal structure of UN is cubic (Fig. 4a) and has $\boldsymbol{Fm\bar{3}m}$ symmetry. Potential products (Fig. 4b-d) of the reaction of UN with H or H_2 have been assessed based on experimentally known compounds,[20] which include U_2N_3 (trigonal crystal with space group $\boldsymbol{P\bar{3}m1}$), U_4N_7 (tetragonal crystal with space group $\boldsymbol{I4cm}$), and UH_3 (cubic crystal with space group $\boldsymbol{Pm\bar{3}n}$). The two primary reactions investigated in this work occur by UN reacting with H_2,

$$\begin{aligned} 6UN + 3H_2 &\rightarrow 2UH_3 + 2U_2N_3 \\ 7UN + \tfrac{9}{2}H_2 &\rightarrow 3UH_3 + U_4N_7, \end{aligned} \tag{1}$$

or H,

$$\begin{aligned} 6UN + 6H &\rightarrow 2UH_3 + 2U_2N_3 \\ 7UN + 9H &\rightarrow 3UH_3 + U_4N_7, \end{aligned} \tag{2}$$

to form UH_3.

The thermodynamic properties, namely the Gibbs free energy G, of the compounds exhibited in Fig. 4, as well as those of H and H_2, are required as a function of temperature to quantify hydrogen-mediated UN decomposition. Although the thermodynamics of H and H_2 gases are well known as a function of temperature and pressure, the dataset for uranium-containing species is less complete. Free energy data is available for UN across a wide temperature range (298 – 2628 K)[35] that encompasses a major portion of the operational temperature range of an NTP fuel element.

By contrast, the thermodynamic data of the nitrogen-rich compounds U_2N_3 and U_4N_7, as well as UH_3 are less complete.[20] In this case, thermodynamics obtained from DFT computations and the QHA approach can augment available experimental data by

providing high-fidelity measures of Gibbs free energy to enable the interrogation of decomposition reactions. Such computations for UN, as plotted in Fig. 5, have been carried out over a wide temperature range (up to 3000 K) and show values that are in quantitative agreement with previous experiments.[35,36] The relative error between computed and experimental values is less than 3% in the temperature range investigated, which provides confidence that DFT-computed thermodynamic quantities can be used to investigate erosion reactions. Similar computations for the compounds of interest show that of the compounds considered, the Gibbs free energy for UN is the lowest, followed by that of U_2N_3, U_4N_7 , and finally UH_3.

The free energetics of the reactions (ΔG_{rxn}) between UN and H to produce U_2N_3 (Fig. 6a) show that decomposition is expected (due to a negative free energy) up to a temperature of ~2000 K. Conversely, the reaction with H_2 is generally not favourable over the entire temperature range examined (300-3000 K). The primary exception is at low temperature, where the free energy of reaction is almost zero, which indicates that the reaction approaches reversibility. The chemical potential μ of H and H_2 may be varied to probe the effect on reaction energies. The chemical potential governs the favourability of hydrogen reaction and can be correlated to the energetics of hydrogen adsorbed on surfaces/into grain boundaries or to the pressure of a gas of hydrogen species. For the present calculations, the chemical potential range corresponds to free energies of gases with pressures ranging from 1 to 8 atm. As pressure (or μ) increases, the reaction free energy curve is shifted to higher temperatures. Effectively, this indicates that higher gas pressure will lead to increased decomposition at higher temperatures.

The reactions that produce U_4N_7 (Fig 6b) exhibit the same general trends noted for U_2N_3: reactions with H_2 do not appear favourable, while those with H are favourable below ~2000 K. In addition, increasing pressure (or μ) from 1 to 8 atm leads to a 500 K

broadening of the thermal decomposition window. The primary difference with U_2N_3 is that the magnitude of the reaction free energy is of much larger scale. The most important implication of this is the stronger thermodynamic driving force for decomposition via H, which could lead to greater UH_3 yield.

The information provided from the analysis of H-UN reactions raises interesting questions concerning mechanisms by which NTP cermet fuel elements may destabilize. Hot atomic hydrogen will diffuse into the tungsten matrix during operation, and, at the end of an operation cycle, the material will cool. As shown from the computations, H will react with UN to form UH_3 when the material cools below 2000 K. Ultimately, these relevance of specific thermodynamic processes will depend on the concentration of hydrogen present in the material, which will in turn be determined by the kinetics of hydrogen diffusion in the specific grain structure of the cermet/cladding.

III.C. Case 3: Fuel Thermal-Mechanical Stability

During operation, a cermet will be subjected to thermal expansion and CTE mismatch stresses and, as described in the previous section, stresses related to chemical reactions of nuclear material with hot hydrogen and the formation of hydrides. The mechanical properties of the metallic matrix to a large extent governs the stress tolerance and fracture behaviour of the element as a whole. In this regard, understanding crystal plasticity and the nature of the high temperature ductile-brittle transition with respect to material characteristics like grain structure and strain rate are critical to developing mechanically stable fuel elements.

In terms of computational approaches to treat mechanics of high-temperature metals, discrete dislocation dynamics simulations provide a first-principles approach to crystal plasticity that is based on dislocation motion and effects like twin formation.[27] In line with the focus on W-UN cermets, tungsten is again used as a benchmark material. A

tungsten polycrystalline microstructure with randomly oriented grains is created using DAMASK with a Voronoi tessellation algorithm (Fig. 7). The average grain diameter is chosen to be 20 microns to roughly mimic that of additively manufactured tungsten.[28] The representative volume element (RVE) is then subjected to uniaxial tension at a strain-rate of 10^{-3} s^{-1}, which is within the standard range of performing laboratory tensile testing, per ASTM standards. Thus, both the material structure and experimental parameters are reflective of laboratory testing conditions.

In the current case, the evolution of stress and strain concentrations at the microstructural level is studied. A maximum strain of 0.05 is obtained after a 50 s simulation. The stress-strain distribution within a room temperature sample (Fig. 7) shows that grain boundaries act as high stress concentration sites, consistent with experimental observation in the literature reporting initiation of materials damage at these sites.[37] Unique to the current modeling approach is that the microscopic stress contour is computed as a direct outcome of discrete dislocation and twinning based crystal plasticity informed by inherent physics of plastic deformation evolution.

The microstructural stress-strain distributions obtained through this approach can be used to derive a system level stress-strain curve (Fig. 8). Doing so results in a stress-strain curve that sees an elastic deformation mechanism transition to a plastic deformation at a strain of 0.0025 (2.5 s). The maximum stress of this system, nominally a pure matrix material, is ~0.35 GPa at the terminal strain of 0.05. If ceramic inclusions were taken into account, we speculate that defects in the matrix material would become pinned by the UN and would lead to higher stiffness and lower tensile strength. Although the microstructure is relatively small, these results are in close accord with room temperature experiments (below the DBTT) obtained for polycrystalline tungsten[37] and thus demonstrate the feasibility of performing simulated experiments on materials based on *ab initio*

techniques.

IV. Conclusions

This work serves as a survey of applications of ICME techniques to W-UN cermets fuel elements for nuclear thermal rockets. Such fuel elements will be exposed to extreme temperatures, beyond those found in nuclear reactors, and hot, high-pressure hydrogen. At such conditions, the material response of cermet fuel elements is complex, and cutting-edge computational materials techniques can be leveraged to aid in qualification and development of high performance fuel materials. In this regard, three important case studies were treated: the interaction of tungsten coating/cladding substrates with hydrogen to interrogate erosion mechanisms, the thermodynamic stability and decomposition of uranium mononitride in the presence of hot hydrogen, and the plasticity of the tungsten cermet matrix.

The simulation results for each of these cases highlighted the close agreement between computed and experimental material properties as well as the ability of computations to supplement experiments. For tungsten erosion, atomistic insight into relative likelihoods of reaction mechanisms and buckling from thermal expansion were evaluated with density functional theory, showing atomic hydrogen events to be the most favourable erosion mechanism. The thermal window where degradation of UN to UH_3 is expected was shown to be at temperatures below 2000 K. This analysis directly relied on density functional theory computations and thermodynamics calculations used to bridge gaps in free energy data and to extrapolate free energies to temperatures beyond those available from experiments. Though here we have calculated the properties of a nominal NTP cermet, these computational methods have wide applicability and can be used to predict the behavior of alternative designs. Finally, microstructure models were employed to perform discrete dislocation dynamics to investigate plasticity. Such computations

provide experimental quality stress-strain curves as well as microstructure-level insight into stress distributions, which can be a powerful aid to understanding high temperature response and the characteristics of a microstructure that leads to desired mechanical properties. While each of these techniques separately shows promise, work is on-going to integrate these techniques into a unified material model of fuel elements, which would greatly aid the certification of fuel element materials for nuclear thermal rockets.

ACKNOWLEDGMENTS

The authors thank NASA's Center Innovation Fund and the NASA Space Technology Mission Directorate (STMD) for sponsoring this work. Resources supporting this work were provided by the NASA High-End Computing (HEC) Program through the NASA Advanced Supercomputing (NAS) Division at Ames Research Center. The authors also thank the creators of imaging software used in this article, OVITO[36] and Paraview[37].

REFERENCES

1. S. K. BOROWSKI, D. R. MCCURDY, T. W. PACKARD, "'7-Launch' NTR Space Transportation System for NASA's Mars Design Reference Architecture (DRA) 5.0," *Proceedings of the 45th AIAA/ASME/SAE/ASEE Joint Propulsion Conference & Exhibit,* Denver, CO, August 2-5, 2009, AIAA (2012).
2. M. G. HOUTS, D. P. MITCHELL, T. KIM, W. J. EMRICH, R. R. HICKMAN, H. P. GERRISH, G. DOUGHTY, A. BELVIN, S. CLEMENT, S. K. BOROWSKI, J. SCOTT, and K. P. POWER, "NASA's Nuclear Thermal Propulsion Project," *Proceedings of the AIAA Space Conference and Exhibition*, Pasadena, CA, August 31-September 2, 2015, AIAA (2015).

3. S. BOROWSI, D. MCCURDY and T. PACKARD, "Nuclear Thermal Propulsion (NTP): A Proven Growth Technology for Human NEO / Mars Exploration Missions," IEEE Aerospace Conference, pp. 1-20, (2012).
4. J. M. NAPIER (ED.), "NERVA Fuel Element Development Program. Summary Report, July 1966- June 1972. Extrusion Studies," *Oak Ridge Y-12 Plant Report* (1972).
5. D. R. KOENIG, "Experience Gained from the Space Nuclear Rocket Program (Rover)," LA-10062-H, Los Alamos National Laboratory (1986).
6. W. D. WILKINSON (ED.), "Nuclear Rocket Program Metallurgy Division Progress Report for Quarter Ending Dec. 31 1964," ANL-7031, Argonne National Laboratory (1965).
7. J. F. COLLINS and D. L. NEWSOM "710 High Temperature Gas Reactor Program Summary Report," GEMP-659, General Electric (1968).
8. M. E. M. STEWART "A Historical Review of Cermet Fuel Development and the Engine Performance Implications," GRC-E-DAA-TN21122, NASA (2015).
9. M. W. BARNES, D. S. TUCKER, and K. M. BENENSKY, "Demonstration of Subscale Cermet Fuel Specimen Fabrication Approach using Spark Plasma Sintering and Diffusion Bonding," *Proceedings of ANS-NETS 2018 – Nuclear and Emerging Technologies for Space*, Las Vegas, NV, February 26-March 1, 2018.
10. D. S. TUCKER, "CERMETS for Use in Nuclear Thermal Propulsion," in *Advances in Composite Materials Development*, IntechOpen (2019).
11. T. AHLGREN et al., "Hydrogen Isotope Exchange in Tungsten during Annealing in Hydrogen Atmosphere," *Nuclear Fusion*, **59**, *2*, 026016 (2019).

12. Z.-G. MEI, M. STAN and B. PICHLET, "First Principles Investigation of Structural, Elastic, Electronic, Vibrational, and Thermodynamic Properties of UN," *Physical Review B*, **84**, 024108 (2011).

13. P. MODAK and A. K. VERMA, "First Principles Investigation of Electronic, Vibrational, Elastic, and Structural Properties of ThN and UN up to 100 GPa," *Physical Review B*, **84**, 024108 (2011).

14. R. ATTA-FYNN and A. K. RAY, "Density Functional Study of the Actinide Nitrides," *Physical Review B*, **76**, 115101 (2007).

15. S. L. WONG, M. MADIVALA, U. PRAHL, F. ROTERS and D. RAABE, "A Crystal Plasticity Model for Twinning- and Transformation-Induced Plasticity," *Acta Materialia*, **118**, 140 (2016).

16. D. CERECEDA, M. DIEHL, F. ROTERS, P. SHANTHRAJ, D. RAABE, J. M. PERLADO and J. MARION, "Linking Atomistic, Kinetic Monte Carlo and Crystal Plasticity Simulations of Single Crystal Tungsten Strength," *GAMM-Mitteilungen*, **38**, 213 (2015).

17. G. KRESSE and J. FURTHMULLER, "Efficient Iterative Schemes for Ab Initio Total-Energy Calculations using a Plane-Wave Basis Set," *Physical Review B*, **54**, 11169 (1996).

18. A. TOGO and I. TANAKA, "First principles phonon calculations in materials science," *Scripta Materialia*, **108**, 1 (2015).

19. J. P. PERDEW, K. BURKE, and M. ERNZERHOF, "Generalized Gradient Approximation Made Simple," *Physical Review Letters*, **77**, 3865 (1996).

20. I. GRENTHE, J. FUGER, R. J. M. KONIGS, R. J. LEMIRE, A. B. MULLER, C. NGUYEN-TRAN, and H. WANNER *Chemical Thermodynamics of*

Uranium, Elsevier Science Publishing Co., Inc., Chap. V, p. 261-279, New York, New York (1992).

21. R. A. EVARESTOV, A. I. PANIN, A. V. BANDURA, and M. V. LOSEV "Electronic Structure of Crystalline Uranium Nitride UN, U_2N_3, and UN_2: LCAO Calculations with the Basis Set Optimization," *Journal of Physics: Conference Series*, **117**, 012015 (2008).

22. K. JUN, J.-U. LEE, M. H. CHANG, and T. ODA "A Comparative Study on Modeling of the Ferromagnetic and Paramagnetic States of Uranium Hydride using a DFT+U Method," *Physical Chemistry Chemical Physics*, **21**, 17628 (2019).

23. J. ANUBHAV, S. P. ONG, G. HAUTIER, W. CHEN, W. D. RICHARDS, S. DACEK, S. CHOLIA, D. GUNTER, D. SKINNER, G. CEDER, and K. A. PERSSON "Commentary: The Materials Project: A Materials Genome Approach to Accelerating Materials Innovation," *APL Materials*, **1**, 011002 (2013).

24. P. SÖDERLIND, A. LANDA, A. PERRON, B. SADIGH, and T. W. HEO "Ground State and Thermodynamical Properties of Uranium Mononitride from Anharmonic First Principles Theory," *Applied Sciences*, **9**, 3914 (2019).

25. R. E. RUNDLE, N. C. BAENZIGER, A. S. WILSON, and R. A. McDonald "The Structure of Carbides, Nitrides, and Oxides of Uranium," *Applied Surface Science*, **70**, 99 (1948).

26. D. GRYAZNOV, E. HEIFETS, and E. KOTOMIN "The First-Principles Treatment of the Electron-Correlation and Spin-Orbital Effects in Uranium Mononitride Nuclear Fuels," *Physical Chemistry Chemical Physics*, **14**, 4482 (2012).

27. F. ROTERS et al., “DAMASK - The Düsseldorf Advanced Material Simulation Kit for Modeling Multi-Physics Crystal Plasticity, Thermal, and Damage Phenomena from the Single Crystal up to the Component Scale,” *Computational Materials Science*, **158**, 420 (2019).

28. J. BRAUN et al., "Molybdenum and tungsten manufactured by selective laser melting: Analysis of defect structure and solidification mechanisms." International Journal of Refractory Metals and Hard Materials 84 (2019): 104999.

29. C. YIN et al., “Tensile properties of baseline and advanced tungsten grades for fusion applications,” *International Journal of Refractory Metals and Hard Materials*, **75**, 153 (2018).

30. D. SMITH et al., “ITER Blanket, Shield Design and Material Data Base,” ITER Documentation Series No. 29, IAEA (1991).

31. A.G. WORTHING, "The Thermal Expansion of Tungsten at Incan-Descent Temperatures,” *Physical Review*, **10**, *6*, 638 (1917).

32. B.N. DUTTA and B. DAYAL, “Lattice Constants and Thermal Expansion of Palladium and Tungsten up to 878°C by X-Ray Method,” *Physica Status Solidi (b)* **3**, *12*, 2253 (1963).

33. P. N. VYUGOV and V. S. GUMENYUK “Thermal Expansion of Tungsten and Tantalum in the Range 1500-3000 ºC,” *High Temp*, **3**, *6*, 879 (1965).

34. R. J. BEALS, J. H. HANDWERK, and B. J. WRONA, "Behavior of Urania–Rare-Earth Oxides at High Temperatures." Journal of the American Ceramic Society 52.11: 578-581, (1969).

35. S. L. HAYES, J. K. THOMAS, and K. L. PEDDICORD “Material Property Correlations for Uranium Mononitride IV. Thermodynamic Properties,” *Journal of Nuclear Materials*, **171**, 300 (1990).

36. F. L. OETTING and J. M. LEITNAKER "The Chemical Thermodynamic Properties of Nuclear Materials I. Uranium Nitride," *Journal of Chemical Thermodynamics*, **4**, 199 (1972).

37. V. KRŠJAK, S. H. WEI, S. ANTUSCH, and Y. DAI "Mechanical Properties of Tungsten in the Transition Temperature Range," *Journal of Nuclear Materials*, **450**, 81 (2013).

38. A. STUKOWSKI, "Visualization and analysis of atomistic simulation data with OVITO – the Open Visualization Tool," Modelling Simul. Mater. Sci. Eng. 18, 015012 (2010).

39. U. AYACHAT, "*The ParaView Guide: A Parallel Visualization Application*," Kitware, ISBN 978-1930934306 (2015).

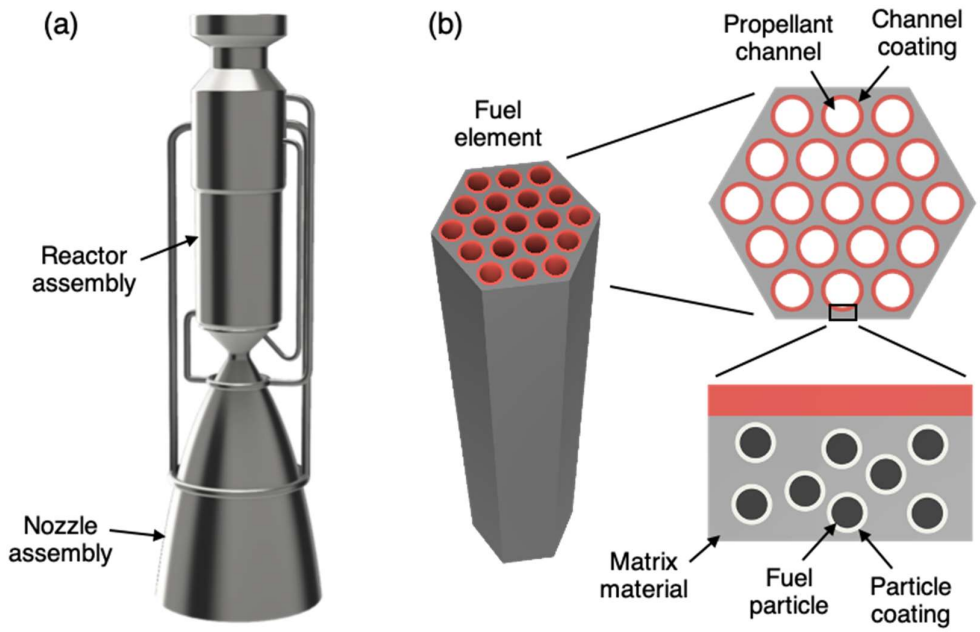

Fig. 1. (a) Depiction of a nuclear thermal rocket. (b) Material configuration of reactor fuel elements.

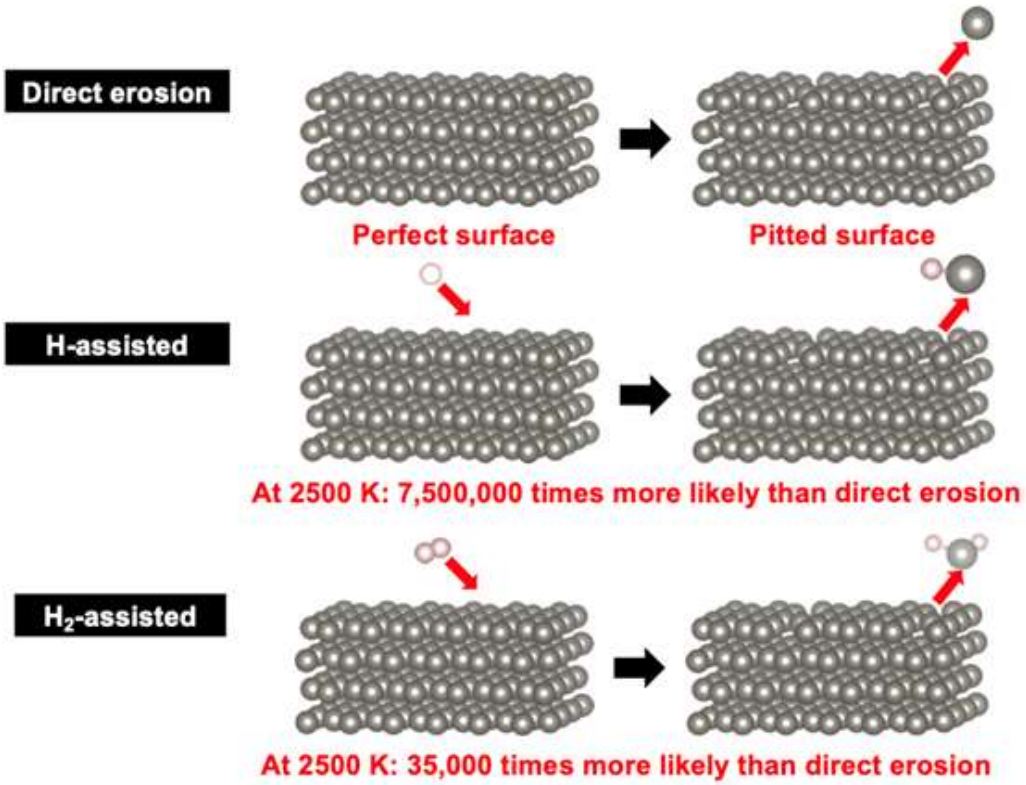

Figure 2. Depiction of hydrogen erosion mechanisms at a tungsten surface and the associated likelihoods based on atomistic modeling.

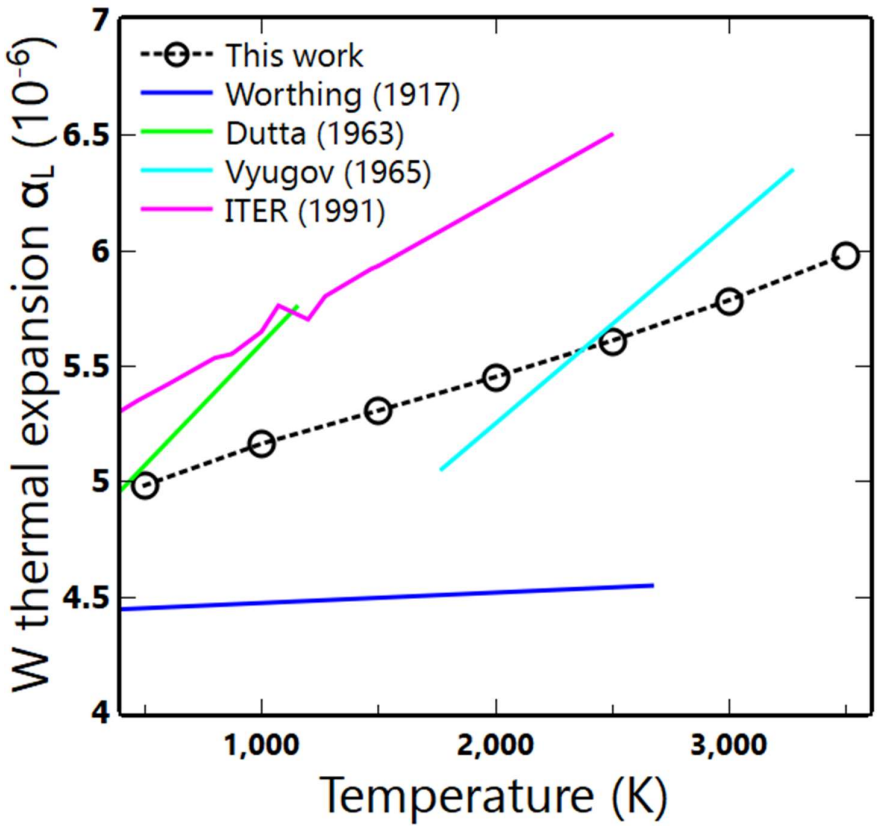

Figure 3. Linear thermal expansion coefficients (a_L) of tungsten calculated from atomistic modeling compared to experiments.[30-33] Computations are provided as a dashed line with open symbols, while the experimental data are provided as solid lines.

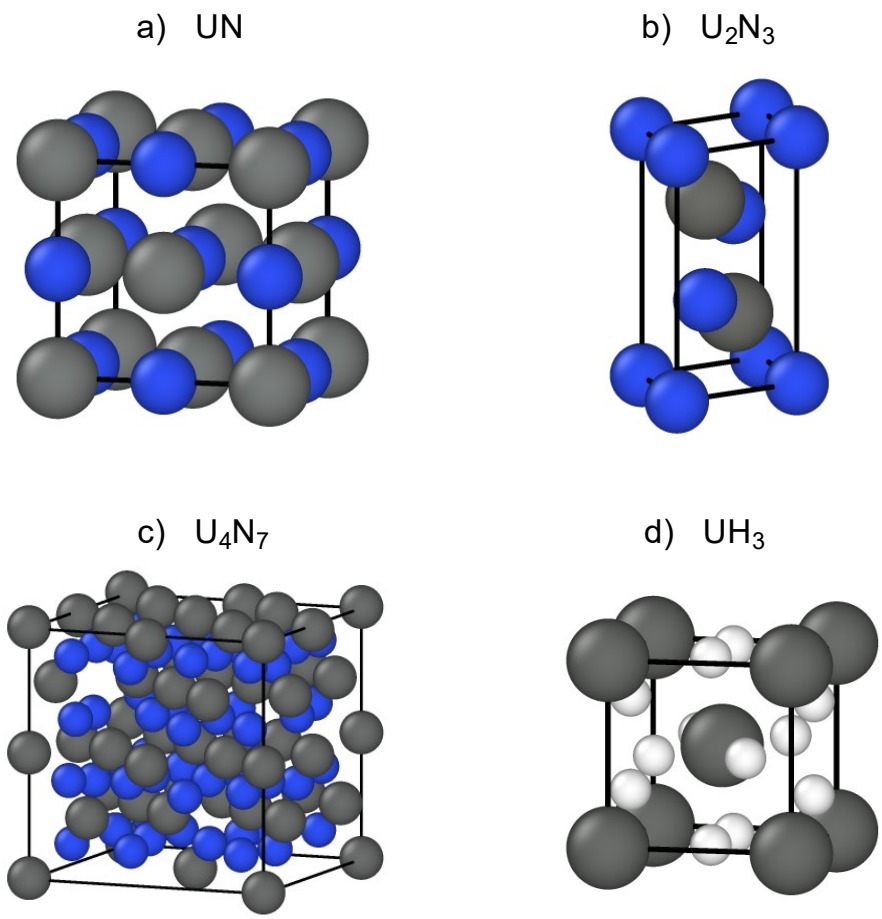

Figure 4. Atomic crystal structures of uranium compounds investigated in this work: (a) uranium mononitride, (b) uranium sesquinitride, (c) tetrauranium heptanitride, and (d) uranium hydride.

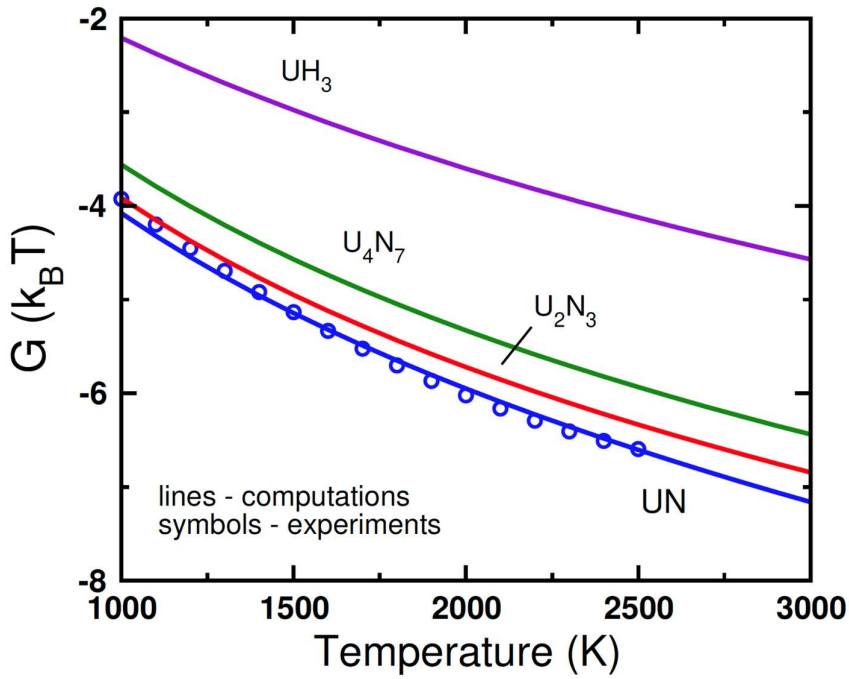

Figure 5. Gibbs free energies per atom (G) of UN, U_2N_3, U_4N_7, and UH_3 as a function of temperature. Computations are provided as solid lines, and experimental data for UN from Hayes et al.[35] are plotted as circles. Free energy is given in thermal units – the product of the Boltzmann constant (k_B) and temperature (T).

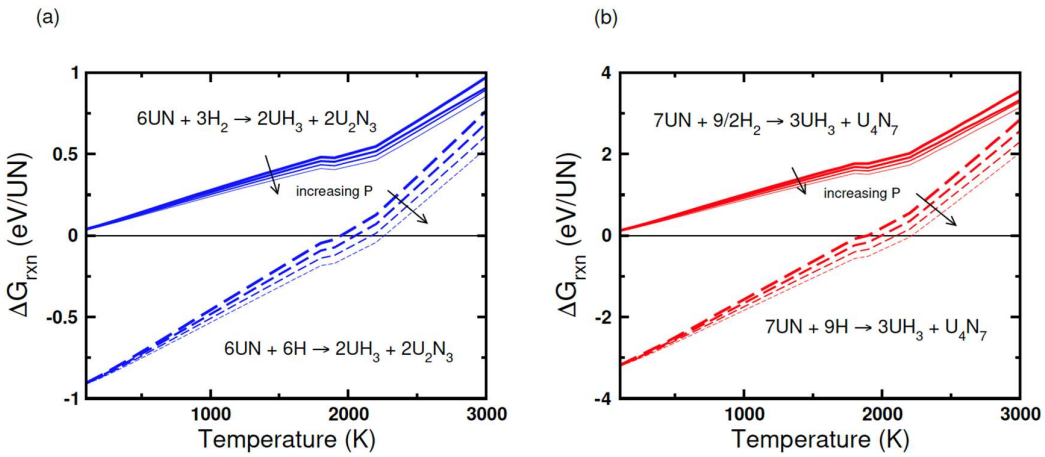

Figure 6. Reaction free energies of UN with H or H_2 to form UH_3 and (a) U_2N_3 or (b) U_4N_7. Reaction free energies are provided as a function of H or H_2 pressure, with arrows indicating increasing pressure from 1 to 8 atm.

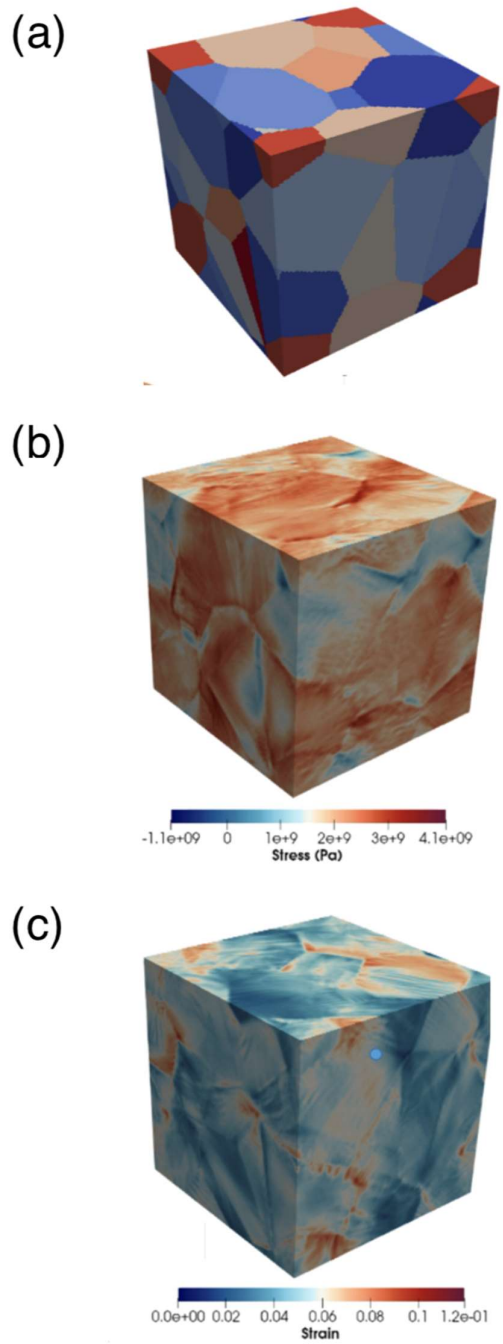

Figure 7. (a) Grain structure of the polycrystalline tungsten representative volume element, (b) stress, and (c) strain of the microstructure mechanical response at 5% global strain. Note that maxima of stress and strain are correlated with grain boundaries and indicate damage that can act as crack initiation sites.

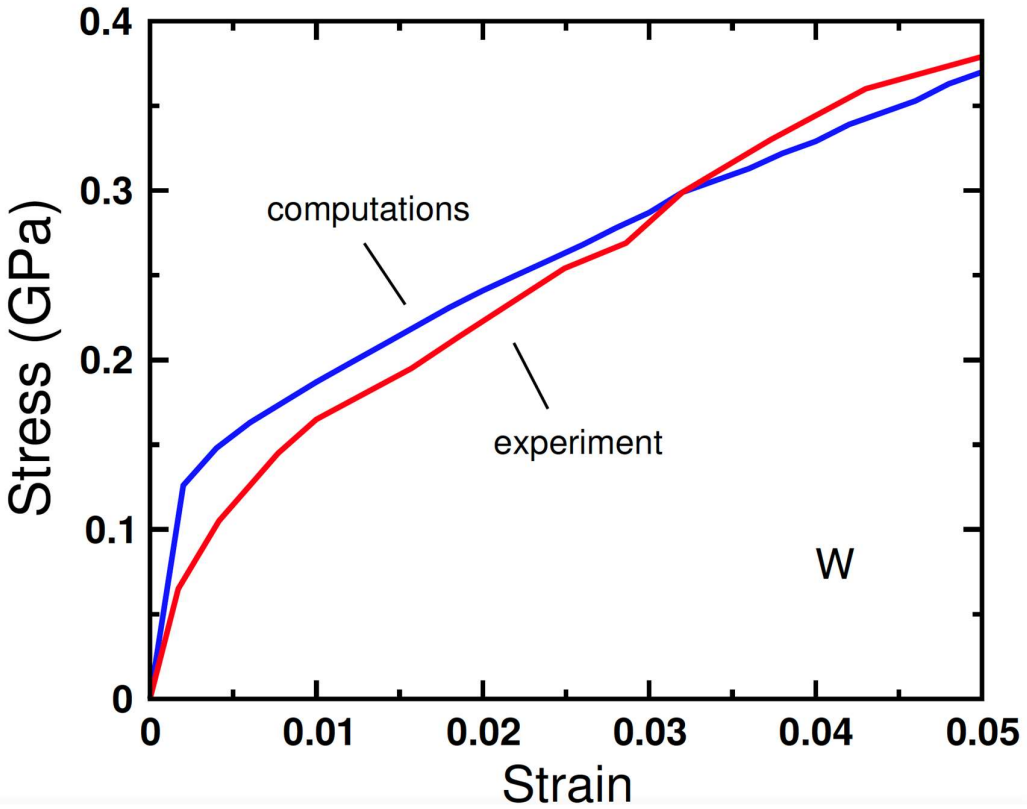

Figure 8. Stress-strain curve of the polycrystalline tungsten representative volume element from room temperature discrete dislocation dynamics simulations and using data from the experiments of Kršjak et al.[37]